Journal of Electrical and Computer Engineering Innovations
(JECEI)
Journal homepage: http://www.jecei.sru.ac.ir

Research paper

Resource Allocation for Full-Duplex Wireless Information and Power Transfer in Wireless Body Area Network

N. Khatami, M. Majidi*

Department of Electrical and Computer Engineering, University of Kashan, Kashan, Iran.

Article Info

Article History:
Received 10 August 2021
Reviewed 26 September 2021
Revised 23 November 2021
Accepted 28 November 2021

Keywords:
Wireless body area network
Simultaneous wireless
Information and power transfer
Full-duplex
Resource allocation
Body energy harvesting
Optimization

*Corresponding Author's Email Address:
m.majidi@kashanu.ac.ir

Abstract

Background and Objectives: The purpose of a wireless body area network (WBAN) is to collect and send vital body signals to the physician to make timely decisions, improve the efficiency of medical informatics systems, and save costs. The sensors of the WBAN network have limited size and energy, and hence, to extend the lifetime of these sensors, they can be powered wirelessly. Our focus in this paper is on a two-tier full-duplex (FD) cooperative WBAN in which sensors, in addition to transmitting physiological information, harvest energy from radio frequency (RF) coordinator signals and body sources. Our goal is to maximize average weighted sum throughput (AWST) under the constraints of each sensor, including meeting the minimum data rate, delay limitation, energy and transmission power constraints.

Methods: The resources allocated to solve this optimization problem are the time slots, the transmission rates of the sensors and coordinator, and the transmission powers of sensors in each time slot. The time scheduling problem in the first step is modeled in the form of a mixed-integer linear programming (MILP) problem and the second step problem is convex. Also, Karush–Kuhn–Tucker (KKT) conditions are presented for power and rate allocation.

Results: In the optimal allocation (OA) mode, contrary to the equal time allocation (ETA) one, with increasing the relay power, the AWST increases despite increasing self-interference (SI). Energy harvesting from the body, nevertheless the power consumption for transmission, makes positive the slope of the instantaneous energy curve for the motion sensor and reduces the corresponding slope for the electrocardiogram (ECG) one. Comparison of the proposed method with previous methods shows that the proposed method has better control over the information flow of sensors, and also in allocating rate to users, fairness is satisfied.

Conclusion: According to the simulation results in our method, the system showed better performance than the equal time allocation mode. We also used the FD technique and with the help of the optimal time scheduling index, we were able to control the SI.

Introduction

Prevention, early detection, and treatment of diseases through the wireless body area networks (WBANs) create a dynamic healthcare system. These real-time networks, which are a new generation of wireless personal area networks (WPANs), include several small devices on the human body or implanted in it.

These nodes convert the body's physiological parameters into electrical signals, and finally, a coordinator collects these signals and sends them to the access point (AP). The collected data is then presented

to the hospital, physician, emergency department, or relatives for tracking the patient's vital signs, emergency actions, awareness of the patient's condition, and updating medical records [1]-[6].

There are two significant challenges associated with WBANs. The first challenge is to provide sustainable power to the body sensors and extend the network's lifetime. The limited capacity of the battery limits the network lifetime. On the other hand, it is difficult to replace and recharge the battery [7]. The authors in [8] have noted that the second challenge is to guarantee the quality of service (QoS) for the delay issue and deliver the data streams of sensors with different priorities. Therefore, in this paper, concerning the importance, the average weighted throughput is considered. By limiting the delay, the loss of critical information should be prevented. The energy needed for the sensors can be provided with the help of simultaneous wireless information and power transfer (SWIPT) technique, and harvesting wireless energy from radio frequency (RF) sources or body energy sources (such as biochemical and biomechanical energy) [9]-[11].

The combined use of SWIPT and relays results in maintaining the connectivity of WBANs, reducing interference, increasing reliability and spectrum and energy efficiency in these networks.

A. Related Works

In [12], a half-duplex (HD) cooperative system that has SWIPT capability with one sensor is investigated. This system aims to find the best relay location to maximize the throughput from the source to the destination. The system model studied in [13] as in [12] is single-sensor and cooperative, where the relay can harvest RF energy from an AP and does not have a buffer. The relay transmits the harvested energy to the sensor and forwards the received information to the AP.

The purpose in [13] is to maximize the information transmission rate under the constraint of the balance between the consumed and harvested energies. Finally, the optimal power splitting ratio and optimal time switching ratio are obtained, and the effect of relay location on system performance is discussed. In [14], a full-duplex (FD) cooperative system with one sensor and one buffer is explained. The continuous transmitted information rate maximization problem in adaptive power allocation mode and constant power allocation mode is formulated. In [15], a cooperative multi-sensor system model is considered, which includes links from sensors to the handset and from the handset to the AP. Also, several sources of RF signal propagation are employed to power WBAN sensors wirelessly and the goal is to maximize the throughput. However, the transmission delay of each user is not taken into account.

The authors are encouraged in [16] and [17] to investigate a cooperative multi-sensor WBAN in which both sensors and relay have energy harvesting, and the goal is to maximize throughput. In both system models, the relay is HD.

In [1], a cooperative multi-sensor WBAN that destination nodes (DNs) and relay node (RN) receive RF energy simultaneously from the source is considered. Power splitting ratio at the relay and each DN are optimization variables. The purpose of the optimization problem is to maximize the information sum-throughput. In [18], a multi-sensor WBAN system model without buffer is expressed in both normal and abnormal states. In the normal mode, the combination of time switching and power splitting is used, but in the abnormal mode, only time switching is used. In the system model of this paper, the coordinator is not considered, and the sensors are in direct contact with the AP, so due to the lack of a coordinator and buffer, it is not possible to control the delay, and sensors must consume more energy to send their information directly to AP.

In [19], a FD cooperative multi-sensor system with buffers is expressed. The purpose is to solve the problem of maximizing average delay limited weighted throughput under the stability of the average queue length in the context of a two-level WBAN architecture. The ability to harvest energy from the body by sensors, constraints on having limited instantaneous buffer length, and having positive instantaneous energy for the sensors are not considered. It should be noted that in all the above papers that have the WBAN system model, harvesting energy from the body and in [1], [8], [15], [16], [20] buffer is not considered.

B. Contribution

In this paper, a two-level multi-sensor WBAN is considered with several sensors, a FD coordinator, and an AP. Sensors send vital information extracted from the body, such as electrocardiograph information, to the coordinator. They can harvest RF wireless energy and body energy, and also, for each sensor, there is a buffer in the coordinator to control the delay of the information of that sensor. The time scheduling of sending different sensors, the transmission rates and powers of the sensors, and the transmission rates of the coordinator are determined Optimally. Resources are allocated to maximize average weighted sum throughput (AWST). Constraints such as the limitation of sensors' transmission powers, delays, and initial sensor energy are considered.

Innovations added to the problem model are as follows:

- In addition to battery-powered sensors, they are

also equipped with RF and body energy harvesting (BEH) system (like mechanical energy).

- To achieve fairness, the average rate of each sensor over all time slots must be greater than a minimum threshold.
- For instantaneous buffer length, a constraint is considered to limit the data transfer delay of each user.
- The time scheduling optimization problem is modeled in the form of mixed-integer linear programming (MILP).
- Allocation of power and rate of each sensor and relay is performed by modeling the problem as a convex one, and to analyze it, Karush–Kuhn–Tucker (KKT) equations are presented.

C. Structure of the Paper

The rest of this paper is as follows: In the next section, we describe the signal and intended system model. Then, we formulate the problem and explain the optimal allocation (OA) and equal time allocation (ETA) modes. After that, the numerical solution and simulation results are presented. The last section concludes the paper.

Signal and System Model

The proposed scenario in Fig. 1, which is a two-level cooperative WBAN, consists of the RN, the source nodes (SNs), and the DN. The FD relay node, called full-duplex relay node (FD-RN), is a decode and forward relay equipped with N first-in-first-out (FIFO) buffers and is responsible for relaying messages to the destination, where *i*th buffer is shown by Q_i. SNs have limited energy, sense the body's physiological signals, and send them to the coordinator. The FD-RN relays the information received from the sensors to the destination, and at the same time, the sensors receive RF energy from that signal. All sensors wirelessly receive RF power from the coordinator, and some sensors can receive energy from the body.

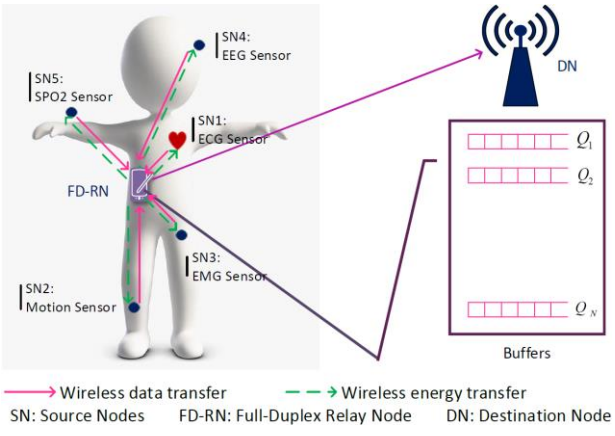

Fig. 1: System model.

The additive white Gaussian noise (AWGN) channel variances in DN and RN are σ_{nD}^2 and σ_{nR}^2, respectively. $h_{sr}^q(j) = \frac{|g_{sr}^q(j)|^2}{\sigma_{nR}^2}$, $h_{rd}(j) = \frac{|g_{rd}(j)|^2}{\sigma_{nD}^2}$, $h_{rr}(j) = \frac{|g_{rr}(j)|^2}{\sigma_{nR}^2}$ are normalized channel gain between *q*th sensor and relay, normalized channel gain between relay and destination, and normalized channel gain of SI at the relay, respectively.

Problem Formulation

According to Shannon's Theorem, the capacity of the channel from the *q*th sensor to the relay and from the relay to the destination in the *j*th time slot is:

$$C_{sr}^{q,l}(j) = W\, log_2\left(1 + \frac{P_s^{q,l}(j)h_{sr}^q(j)}{P_r^{q,l}(j)h_{rr}(j)+1}\right), \forall q,l,j \quad (1)$$

$$C_{rd}^{q,l}(j) = W\, log_2\left(1 + P_r^{q,l}(j)h_{rr}(j)\right), \forall q,l,j, \quad (2)$$

where the channel capacity of *q*th-RN and RN-DN are $C_{sr}^{q,l}(j)$ and $C_{rd}^{q,l}(j)$, respectively. Also, W and *q* and *l* are bandwidth, and sensor number and buffer number, and $P_s^{q,l}(j)$ is the power of the sensor in the *j*th time slot as *q*th sensor is sending data to the relay, and at the same time, *l*th buffer is emptying from the relay to its destination. $P_r^{q,l}(j)$ is the power of the relay in the *j*th time slot. We assume $m_{q,l}(j)$ as a binary time scheduling variable where if it is one, it indicates that in *j*th time slot data from *q*th sensor is being sent to the relay and from *l*th buffer is leaving towards AP [21], [22]. In any time slot *j*, only one sensor is allowed to send, and only the data of one buffer can be read and sent from the relay.

$$\sum_{q=1}^{N}\sum_{l=1}^{N} m_{q,l}(j) = 1, \forall j \quad (3)$$

$$m_{q,l}(j) \in \{0,1\}, \forall q,l,j \quad (4)$$

$$E_q(j) = E_q(j-1) - \sum_{l=1}^{N} m_{q,l}(j)\, P_s^{q,l}(j)\, \tau + E_{BH}(q)$$

$$+ \sum_{k=1,k\neq q}^{N}\sum_{l=1}^{N} m_{k,l}(j)\, P_r^{k,l}(j)\, \tau\, \eta\, \left|g_{sr}^q(j)\right|^2, \forall q,j, \quad (5)$$

where $E_q(j)$ is the energy of the *q*th sensor in the time slot *j*, $E_{BH}(q)$ is the amount of energy harvested from the body by the *q*th sensor, τ is the length of each time slot, and η is the energy conversion efficiency of the sensor.

The energy limitation of the *q*th sensor means that the total energy consumption of that sensor must be less than the total energy that is harvested from the RF and the body, plus its primary energy as follows:

$$\sum_{j=1}^{J}\sum_{l=1}^{N} m_{q,l}(j)\, P_s^{q,l}(j)\, \tau \le \sum_{j=1}^{J}\sum_{k=1,k\neq q}^{N}\sum_{l=1}^{N} m_{k,l}(j) P_r^{k,l}(j)\, \eta\, \left|g_{sr}^{q}(j)\right|^2 \tau + E_0 + JE_{BH}(q), \forall q, \quad (6)$$

where E_0 is the initial energy of each sensor. The instantaneous energy of each sensor is positive:

$$0 \le E_q(j), \forall q, j. \quad (7)$$

$B_q(j)$ is *q*th buffer length in the time slot *j*. Also, the length of the buffer cannot be negative, and BF^{max} is the maximum value of the buffer length, hence

$$B_q(j) = B_q(j-1) - \sum_{k=1}^{N} \tau R_{rd}^{k,q}(j) + \sum_{l=1}^{N} \tau R_{sr}^{q,l}(j), \forall q, j \quad (8)$$

$$0 \le B_q(j), \forall q, j \quad (9)$$

$$B_q(j) \le BF^{max}, \forall q, j \quad (10)$$

$$\frac{1}{J}\sum_{j=1}^{J}\sum_{l=1}^{N} R_{sr}^{q,l}(j) \le \frac{1}{J}\sum_{j=1}^{J}\sum_{k=1}^{N} R_{rd}^{k,q}(j), \forall q, \quad (11)$$

$R_{sr}^{q,l}(j)$ indicates transmission rate from the *q*th sensor to the relay in the *j* time slot when the *l*th buffer at the relay gets empty to send its information towards the destination. Also, $R_{rd}^{k,q}(j)$ is the transmission rate when the *k*th sensor is active and *q*th buffer sends its information from the relay to the destination in the time slot *j*. Equation (11) is written because buffers do not waste data, and data queues are stable. Transmission rates cannot exceed channel capacity, therefore:

$$R_{sr}^{q,l}(j) \le W m_{q,l}(j)\, log_2\left(1 + \frac{P_s^{q,l}(j) h_{sr}^{q}(j)}{P_r^{q,l}(j) h_{rr}(j)+1}\right), \forall q, l, j \quad (12)$$

$$R_{rd}^{q,l}(j) \le W m_{q,l}(j)\, log_2\left(1 + P_r^{q,l}(j) h_{rd}(j)\right), \forall q, l, j. \quad (13)$$

To ensure fairness among the sensors, the average rates must be higher than a minimum.

$$R_{min}^{q} \le \frac{1}{J}\sum_{j=1}^{J}\sum_{l=1}^{N} R_{sr}^{q,l}(j), \forall q. \quad (14)$$

The following is a short-term constraint for power $P_s^{q,l}(j)$:

$$0 \le P_s^{q,l}(j) \le P_s^{max}, \forall q, l, j, \quad (15)$$

where P_s^{max} is the maximum transmit power. It should be noted that $P_r^{q,l}(j)$ is assumed to be equal to P_r^{max}.

The difference between OA mode and ETA is that in OA mode, we determine $m_{q,l}(j)$ optimally by solving the optimization problem according to the constraints in our first step. However, in ETA mode, $m_{q,l}(j)$ is predefined.

A. OA mode

In OA mode, the allocation of scheduling power, sensor transmission rate, and relay transmission rate are dynamic. Our purpose is to maximize AWST. $m_{q,l}(j)$, $P_s^{q,l}(j)$, $R_{sr}^{q,l}(j)$ and $R_{rd}^{q,l}(j)$ are the optimization variables. Since $m_{q,l}(j)$ is a binary optimization variable, and the other variables are real, according to constraints such as (12), the problem is mixed-integer nonlinear programming (MINLP) and non-convex. Hence, we consider the following two steps to solve it.

In the first step, we assume that $P_s^{q,l}(j)$ is equal to the constant value P_s^{max}. Then we get $m_{q,l}(j)$. Therefore, $m_{q,l}(j)$, $R_{sr}^{q,l}(j)$ and $R_{rd}^{q,l}(j)$ are the optimization variables of this step and the optimization problem is as follows:

P1: $\max \frac{1}{J}\sum_{j=1}^{J}\sum_{q=1}^{N}\sum_{l=1}^{N} W_q\, R_{sr}^{q,l}(j)$

s.t. a) $\sum_{q=1}^{N}\sum_{l=1}^{N} m_{q,l}(j) = 1, \forall q$

b) $m_{q,l}(j) \in \{0,1\}, \forall q, l, j$

c) $E_q(j) = E_q(j-1) - \sum_{l=1}^{N} m_{q,l}(j) P_s^{max}\, \tau + \sum_{k=1,k\neq q}^{N}\sum_{l=1}^{N} m_{k,l}(j) P_r^{max}\, \tau\, \eta\, \left|g_{sr}^{q}(j)\right|^2 + E_{BH}(q), \forall q, j$

d) $\sum_{j=1}^{J}\sum_{l=1}^{N} m_{q,l}(j)\, P_s^{max} \tau \le \sum_{j=1}^{J}\sum_{k=1,k\neq q}^{N}\sum_{l=1}^{N} m_{k,l}(j) P_r^{max}\, \tau\, \eta\, \left|g_{sr}^{q}(j)\right|^2 + E_0 + JE_{BH}(q), \forall q$

e) $0 \le E_q(j), \forall q, j$

f) $B_q(j) = B_q(j-1) - \sum_{k=1}^{N} \tau R_{rd}^{k,q}(j) + \sum_{l=1}^{N} \tau\, R_{sr}^{q,l}(j), \forall q, j$

g) $0 \le B_q(j), \forall q, j$

h) $B_q(j) \le BF^{max}, \forall q, j$

i) $\frac{1}{J}\sum_{j=1}^{J}\sum_{l=1}^{N} R_{sr}^{q,l}(j) \le \frac{1}{J}\sum_{j=1}^{J}\sum_{k=1}^{N} R_{rd}^{k,q}(j), \forall q$

j) $R_{sr}^{q,l}(j) \le W m_{q,l}(j).\ log_2\left(1 + \frac{P_s^{max} h_{sr}^{q}(j)}{P_r^{max} h_{rr}(j)+1}\right), \forall q, l, j$

k) $R_{rd}^{q,l}(j) \le W m_{q,l}(j).\ log_2\left(1 + P_r^{max}\, h_{rr}(j)\right), \forall q, l, j$

l) $R_{min}^{q} \le \frac{1}{J}\sum_{j=1}^{J}\sum_{l=1}^{N} R_{sr}^{q,l}(j), \forall q.$

Because this problem contains integer and continuous variables and also functions are affine, it is a MILP.

In the second step, we consider $m_{q,l}(j)$ obtained from the first step to be known. $R_{sr}^{q,l}(j)$, $P_s^{q,l}(j)$, $R_{rd}^{q,l}(j)$

are optimization variables and the resulting problem, according to the objective function and constraints, is convex as follows:

$$\text{P2: } \max \frac{1}{J}\sum_{j=1}^{J}\sum_{q=1}^{N}\sum_{l=1}^{N} W_q\, R_{sr}^{q,l}(j)$$

s.t : c,d,e,f,g,h,i,j,k,l

m) $P_s^{q,l}(j) \le P_s^{max}, \forall q,l,j$

n) $0 \le P_s^{q,l}(j), \forall q,l,j$

To solve problem P2, CVX software can be used. The whole problem-solving process is presented in Algorithm 1 in two steps.

Algorithm 1. Solution of OA mode problem

1. **Initialization**: P_s^{max},P_r^{max}, R_{min}^{q} , and BF^{max}
   Number of sensors and buffers.
   Number of time slots.
   Duration of each time slots.
   Energy conversion efficiency.
   Weight of each SN (User Priorities).
   Initial energy of each SN.
2. **First optimization step :**
   Solve optimization problem P1.
   Output: $m_{q,l}(j)$.
3. **Second optimization step :**
   $m_{q,l}(j)$ is determined from first step.
   Solve optimization problem P2.
   Output: $P_s^{q,l}(j), R_{sr}^{q,l}(j)$ and $R_{rd}^{q,l}(j)$.

For the analytical solution of the second step, we can write KKT conditions [23], [24]. To do so, first, consider the Lagrangian function of problem P_2 as follows.

$$\sum_{j=1}^{J} L_j\left(P_s^{q,l}(j), R_{sr}^{q,l}(j), R_{rd}^{q,l}(j), \varphi, \mu, \zeta, \nu, o, \rho, \lambda, \alpha, \beta, \delta, \psi, \varepsilon\right)$$
$$= -\frac{1}{J}\sum_{j=1}^{J}\sum_{q=1}^{N}\sum_{l=1}^{N} W_q\, R_{sr}^{q,l}(j) +$$
$$\sum_{j=1}^{J}\sum_{q=1}^{N}\varphi_q(j)[E_q(j) - E_q(j-1) + \sum_{l=1}^{N} m_{q,l}(j)P_s^{q,l}(j)\tau$$
$$-E_{BH}(q) - \sum_{k=1,k\neq q}^{N}\sum_{l=1}^{N} m_{k,l}(j)P_r^{max}\eta\left|g_{sr}^{q}(j)\right|^2\tau] +$$
$$\sum_{j=1}^{J}\sum_{q=1}^{N}\mu_q[\sum_{l=1}^{N} m_{q,l}(j)\, P_s^{q,l}(j)\tau - \frac{E_0}{J} -$$
$$\sum_{k=1,k\neq q}^{N}\sum_{l=1}^{N} m_{k,l}(j)P_r^{max}\eta\left|g_{sr}^{q}(j)\right|^2\tau - E_{BH}(q)] +$$
$$\sum_{j=1}^{J}\sum_{q=1}^{N}\zeta_q(j)[-E_q(j)] + \sum_{j=1}^{J}\sum_{q=1}^{N}\nu_q(j)[B_q(j) -$$
$$B_q(j-1) + \tau\sum_{k=1}^{N} R_{rd}^{k,q}(j) - \tau\sum_{l=1}^{N} R_{sr}^{q,l}(j)] +$$
$$\sum_{j=1}^{J}\sum_{q=1}^{N} o_q(j)[-B_q(j)] + \sum_{j=1}^{J}\sum_{q=1}^{N}\rho_q(j)[B_q(j) -$$
$$BF^{max}] + \sum_{j=1}^{J}\sum_{q=1}^{N}\lambda_q[\sum_{l=1}^{N} R_{sr}^{q,l}(j) -$$
$$\sum_{j=1}^{J}\sum_{q=1}^{N}\sum_{l=1}^{N}\alpha_{q,l}(j)[R_{sr}^{q,l}(j) - Wm_{q,l}(j)log_2(1 +$$
$$\frac{P_s^{q,l}(j)h_{sr}^{q}(j)}{P_r^{max}h_{rr}(j)+1})] + \sum_{j=1}^{J}\sum_{q=1}^{N}\sum_{l=1}^{N}\beta_{q,l}(j)\left[R_{rd}^{k,q}(j) -\right.$$
$$\left.Wm_{q,l}(j)\, log_2\left(1 + P_r^{max}h_{rd}(j)\right)\right] +$$
$$\sum_{j=1}^{J}\sum_{q=1}^{N}\delta_q\left[R_{min}^{q} - \sum_{l=1}^{N} R_{sr}^{q,l}(j)\right] +$$
$$\sum_{j=1}^{J}\sum_{q=1}^{N}\sum_{l=1}^{N}\psi_{q,l}(j)\left[P_s^{q,l}(j) - P_s^{max}\right] +$$
$$\sum_{j=1}^{J}\sum_{q=1}^{N}\sum_{l=1}^{N}\varepsilon_{q,l}(j)\left[-P_s^{q,l}(j)\right],$$

where φ, μ, ζ, ν, o, ρ, λ, α, β, δ,ψ,ε are Lagrange multipliers. To achieve the KKT conditions, we follow below four items:

1) Conditions C_1 to C_{12} must be met.

2) The Lagrangian multipliers of unequal constraints must all be positive.

$$\mu \ge 0, \zeta \ge 0, o \ge 0, \rho \ge 0, \lambda \ge 0, \alpha \ge 0, \beta \ge 0, \delta \ge 0,$$
$$\psi \ge 0, \varepsilon \ge 0$$

3) For each of the optimization variables, a partial derivative is taken. The gradient of the Lagrange function must be equal to zero.

$$G_1: \frac{\partial L}{\partial P_s^{q,l}(j)} = \sum_{j=1}^{J}\mu_q\, m_{q,l}(j)\,\tau +$$
$$\sum_{j=1}^{J}\varphi_q(j)m_{q,l}(j)\,\tau - \sum_{j=1}^{J}\alpha_{q,l}(j)Wm_{q,l}(j)$$
$$\left[\frac{h_{sr}^{q}(j)}{\left(P_r^{max}h_{rr}(j)+1\right)+\left(P_s^{q,l}(j)h_{sr}^{q}(j)\right)ln2}\right] +$$
$$\sum_{j=1}^{J}\psi_{q,l}(j) - \sum_{j=1}^{J}\varepsilon_{q,l}(j) = 0$$
$$G_2: \frac{\partial L}{\partial R_{sr}^{q,l}(j)} = -\frac{1}{J}\sum_{j=1}^{J} W_q - \sum_{j=1}^{J}\nu_q(j)\;\tau +$$
$$\sum_{j=1}^{J}\lambda_q + \sum_{j=1}^{J}\alpha_{q,l}(j) - \sum_{j=1}^{J}\delta_q = 0$$
$$G_3: \frac{\partial L}{\partial R_{rd}^{q,l}(j)} = \sum_{j=1}^{J}\nu_l(j)\;\tau - \sum_{j=1}^{J}\lambda_l +$$
$$\sum_{j=1}^{J}\beta_{q,l}(j) = 0$$

4) First, we have to rewrite the inequality constraint functions to the standard form fi(x) ≤ 0, where fi (x) is the ith inequality constraint function [23]. The Complementary slackness conditions are written as follows:

$$CS1: \mu_q[\sum_{j=1}^{J}\sum_{l=1}^{N} m_{q,l}(j)P_s^{q,l}(j)\,\tau -$$
$$\sum_{j=1}^{J}\sum_{k=1,k\neq q}^{N}\sum_{l=1}^{N} m_{k,l}(j)P_r^{max}\;\eta\left|g_{sr}^{q}(j)\right|^2\tau$$
$$-E_0 - JE_{BH}(q)] = 0$$
$$CS2: \lambda_q[\sum_{j=1}^{J}\sum_{l=1}^{N} R_{sr}^{q,l}(j) - \sum_{j=1}^{J}\sum_{k=1}^{N} R_{rd}^{k,q}(j)] = 0$$
$$CS3: \alpha_{q,l}(j)\left[R_{sr}^{q,l}(j) - Wm_{q,l}(j)log_2\left(1 + \frac{P_s^{q,l}(j)h_{sr}^{q}(j)}{P_r^{max}h_{rr}(j)+1}\right)\right] = 0$$
$$CS4: \beta_{q,l}(j)\left[R_{rd}^{k,q}(j) - Wm_{q,l}(j)\, log_2(1 + P_r^{max}h_{rd}(j))\right] = 0$$
$$CS5: \psi_{q,l}(j)\left[P_s^{q,l}(j) - P_s^{max}\right] = 0$$
$$CS6: \varepsilon_{q,l}(j)\left[-P_s^{q,l}(j)\right] = 0$$
$$CS7: \delta_q\left[R_{min}^{q} - \frac{1}{J}\sum_{j=1}^{J}\sum_{l=1}^{N} R_{sr}^{q,l}(j)\right] = 0$$
$$CS8: \rho_q(j)\left[B_q(j) - BF^{max}\right] = 0$$
$$CS9: \zeta_q(j)\left[-E_q(j)\right] = 0$$
$$CS10: o_q(j)[-B_q(j)] = 0$$

With the help of Newton's method, the set of KKT equations can be solved, and the optimal point can be obtained.

B. ETA Mode

In ETA mode, we assign equal access times to the sensors, and the sensors change their turn rotationally. Given that $m_{q,l}(j)$ is definite and static in this case, and the ETA optimization problem is similar to the P2 problem. This case was proposed for comparison with the performance of the optimal OA mode.

Simulation Results and Discussion

Using MATLAB software and CVX software, we solve the problems of OA and ETA modes and analyze the results. In the simulations, we have considered one electrocardiogram (ECG) and one motion sensor. The parameters used in the simulations are described in Table 1. To model the channel, the Lognormal distribution is most compatible with dynamic scenarios [25], [26]. Therefore, here too, we use the Lognormal distribution to implement the channel model between the sensors and the coordinator.

$h_{ij}[\mathrm{dB}] \sim N(\mu_{ij}, \sigma_{ij})$

We take the distribution parameters, i.e., μ_{ij} (mean) and σ_{ij} (variance), from the information in Table 2 [20]. In addition to the random Lognormal distribution, $P_{ij}[dB]$, which is the relative power loss of the link between transmitter *j* and receiver *i*, is also considered. d_{ij} is the distance between the transmitter *j*, and the receiver *i*. *j* indicates coordinator, and *i* is the body's sensor. $h_{ij}[dB]$ and $P_{ij}[dB]$ are added together.

For the channel gain model between the coordinator node and the base station, we use $h = {}^{200}/_{d^4}$,where *d* is the distance between those two nodes with a uniform distribution between 50 to 200 meters.

Table 1: Simulation parameters

Parameter	Symbol	Value
Number of sensors and buffers	N	2
Number of time slots	J	20
Channel bandwidth [19]	B	10 kHz
Duration of each time slot	τ	20 ms
Noise power at the RN [19]	σ_{nR}^2	-124 dBm
Noise power at the DN [19]	σ_{nD}^2	-124 dBm
Energy conversion efficiency [19]	η	0.8
Maximum power of sensors [19]	P_s^{max}	0.1mW
Maximum power of relay [19]	P_r^{max}	1 mW
Array of weight of each Sensor (User Priorities) [27]	W	$(2/11) \times [6,5]$
Carrier frequency [28]	f_c	4.2 GHz
Energy harvesting by ECG sensor [29]	$E_{BH}(1)$	4 µJ
Energy harvesting by Motion sensor [30]	$E_{BH}(2)$	0.4 µJ
Maximum length of the buffer	BF^{max}	20 Kbit

Table 2: Channel parameters between sensors and synchronizer [20]

Location of sensor	$\boldsymbol{P_{ij}[dB]\backslash d_{ij}[cm]}$	$\boldsymbol{\mu_{ij}\backslash\sigma_{ij}}$
chest	-43.29\26	-0.72\2.67
right foot	-51.00\92	-3.25\6.21

In Fig. 2, the instantaneous rates of the first and second sensors are plotted according to the time slot number. In this case, the initial energy value E_0 varies from 10 microjoules to 400 microjoules. Fig. 2 shows that in the OA mode, the sensor allocates more time slots to itself due to its higher weight and better channel condition. The time scheduling index is such that one of the sensors must be sent in a time slot, so the diagrams in Fig. 2 are also based on complementary time slots.

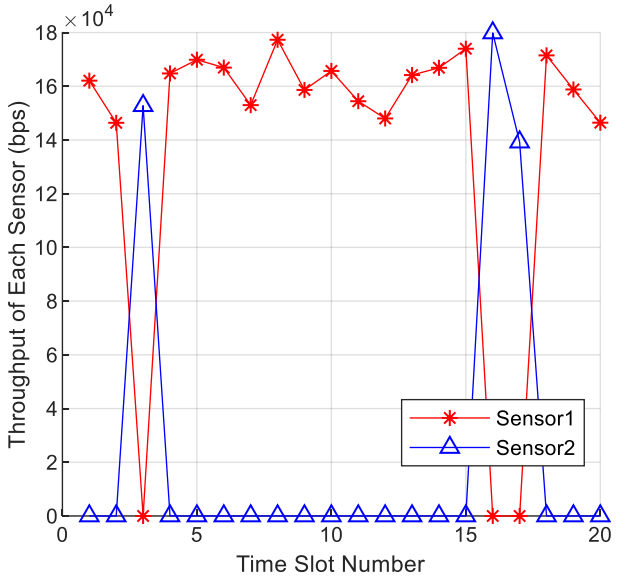

Fig. 2: Instantaneous rate of the first and second sensors according to the time slot number.

Flowchart 1 is based on Algorithm 1. Only a loop is added to perform z_0 Monte Carlo simulations. We use Flowchart 1 for calculating AWST.

Fig. 3 shows the mean weighted throughputs of the first and second sensors in terms of initial energy E_0. When the initial energy of the sensors is low, they can send with less power. Hence, they have lower mean weighted throughputs. By increasing the initial energy, the sensors can send at their maximum power, so their mean weighted throughputs go up and reach saturation.

As a result, the mean weighted throughput of the first sensor (ECG) reaches a maximum of 140 Kbps due to higher weight and better channel condition, and the mean weighted throughputs of the second sensor (Motion) reaches a maximum of 20 Kbps due to lower rate weight and worse channel condition.

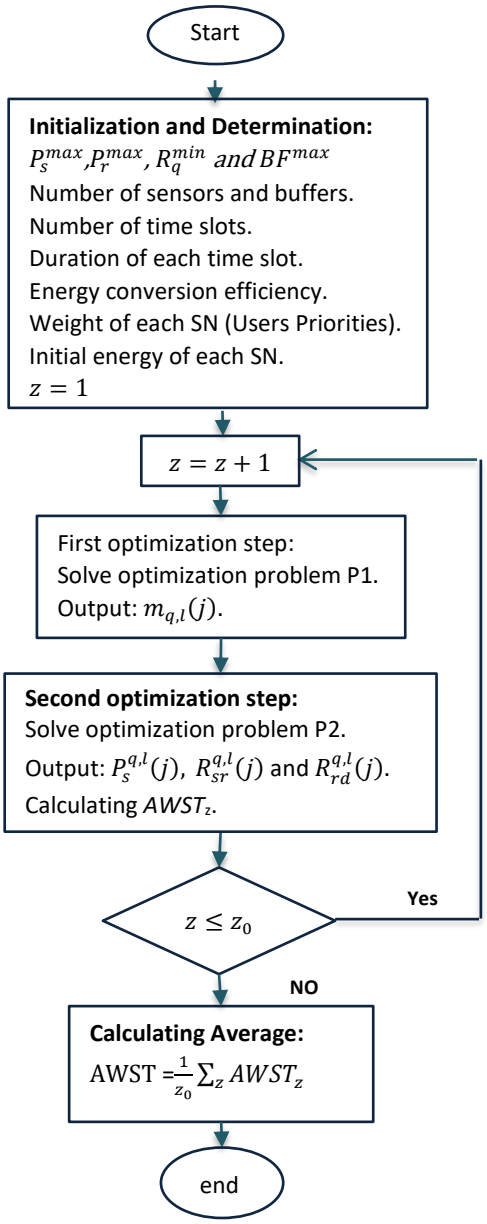

Flowchart 1: Monte Carlo simulation for calculating AWST.

Fig. 4, Fig. 5, and Fig. 6 show the AWST comparisons for OA and ETA modes. In Fig. 4, the AWST is plotted in terms of the initial energy E_0. When the initial energy of the sensors is small, they cannot send a large percentage of their maximum power, so the throughput is low, and the AWST is also low. As the initial energy increases, the sensors can transmit at a higher percentage of their maximum power; as a result, the diagram goes up. By increasing E_0, the sensors can send P_s^{max} at their maximum power; consequently, AWST reaches its maximum value, and the graph goes to saturation. By comparing the two diagrams for the OA and ETA modes, it can be seen that at the initial energy of 100 micro joules, the AWST value in OA mode is 6.85% higher than in ETA mode.

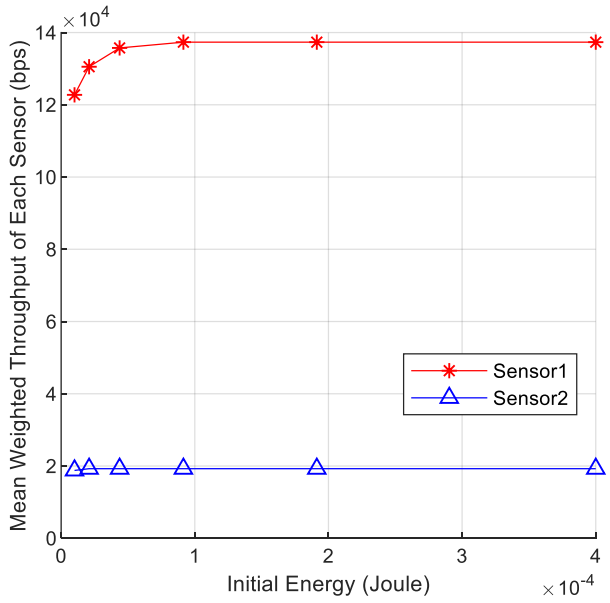

Fig. 3: Comparison of the mean weighted throughput of the first and second sensors in terms of initial energy.

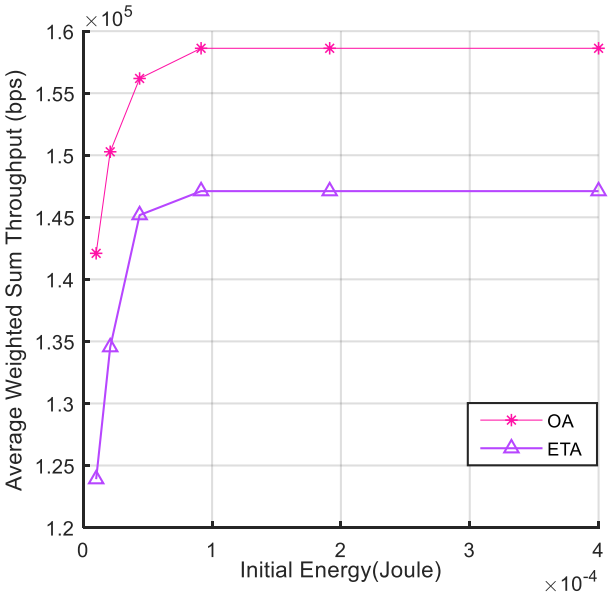

Fig. 4: Comparison of AWST diagrams in E_0 for both OA and ETA modes.

Fig. 5 shows the AWST in terms of different h_{rr} for the OA and ETA modes. In this case, the initial energy value is 200 microjoules. Initially, h_{rr} is very small, and its power can be ignored compared with the power of noise at the denominator of the Shannon relationship. By increasing the h_{rr} at the denominator of the Shannon relationship, the amount of self-interference (SI) power of the FD relay becomes significant, resulting in a decrease in throughput and AWST. It can be seen that in h_{rr}=-140 dB, AWST in OA mode is 10 Kbps higher than ETA mode.

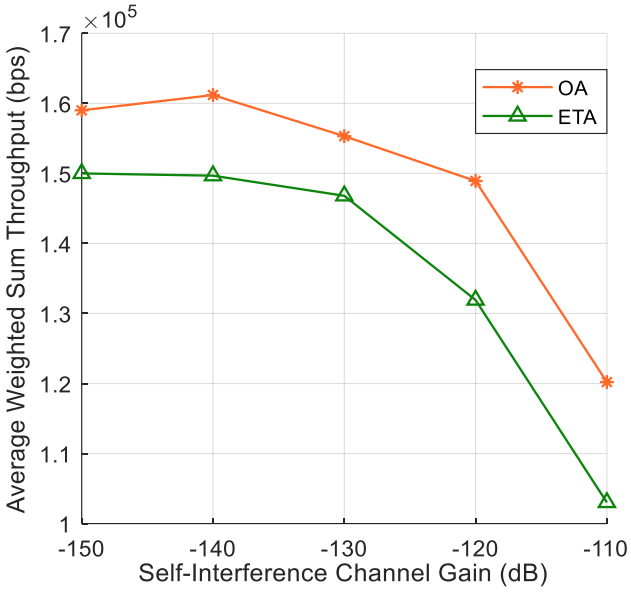

Fig. 5: Comparison of AWST diagrams in h_{rr} for OA and ETA modes.

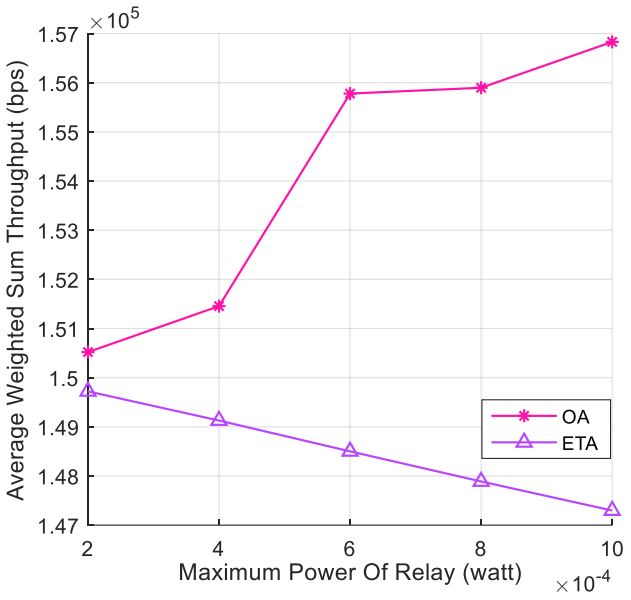

Fig. 6: Comparison of AWST diagrams in terms of P_r^{max} for OA and ETA modes.

In Fig. 6 AWST for different P_r^{max} the diagrams of the OA and ETA modes are compared. According to Fig. 6, for the OA mode, when P_r^{max} increases, the capacity of the relay-destination channel increases; hence the buffers in the relay may have a higher output rate. It causes the total rate of the sensors to relay to increase, but with increasing P_r^{max}, the diagram slope decreases because increasing P_r^{max} also increases SI. For the ETA mode, we see that the AWST is decreasing because only half of the time slots are allocated to the first sensor (ECG), which has a higher weight rate, and the number of its time slots cannot be increased. On the other hand, with the increase in P_r^{max}, the SI is also increasing, which leads to a decrease in AWST.

Therefore, in contrast to the OA mode, which can allocate more time slots to the ECG sensor and increase the total rate, in the ETA mode, it is impossible to increase the rate.

Fig. 7 shows AWST in terms of E_0 for sitting position, walking mode, and no BEH. In the small E_0s, the AWST of the walking mode is higher than the sitting position and the non-harvested mode.

At larger E_0s, the initial energy is saturated, and the increase in E_0 no longer has an effect on the increase in throughput, so all three curves are getting closer to each other. For validation, we compared the method of [19] with our method. In Fig. 8, Fig. 9, and Fig. 10, BF^{max}= 5 Kbit and R_{min}=40 Kbps.

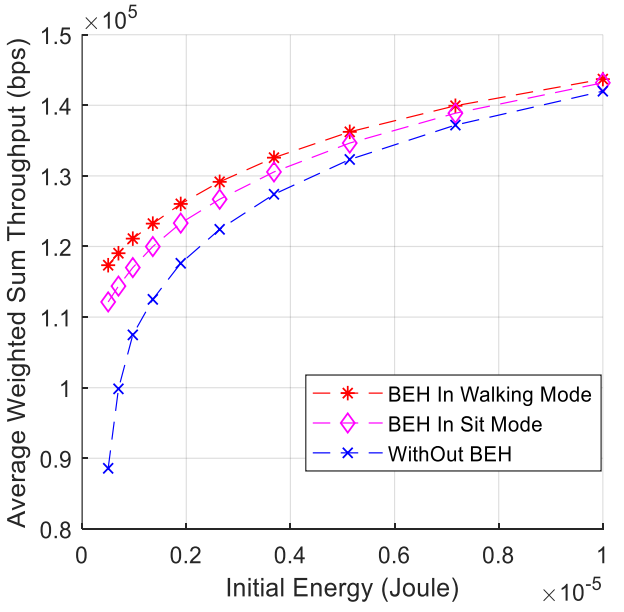

Fig. 7: Comparison of AWST diagrams for walking, sitting, and without energy harvesting modes.

Fig. 8 shows filled buffer length of the first and second sensors in terms of time slot numbers, and the initial energy value E_0 is 100 microjoules. In our method, we defined the threshold (BF^{max}=5 Kbit), which controls the filled length of the buffers, but in the method of [19], there is no threshold, so their buffers have overflowed.

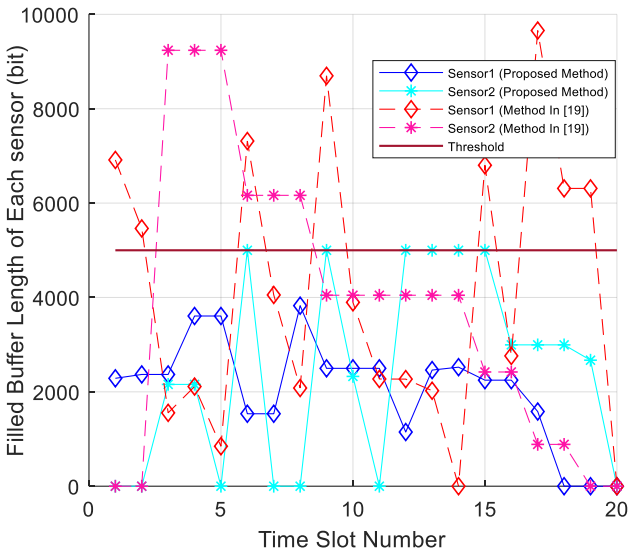

Fig. 8: Filled buffer lengths of the sensors in terms of time slot numbers to compare the proposed method with [19].

As can be seen in Fig. 9, the fairness is not satisfied in [19], because the rate of sensor 2 is zero and lower than threshold (R_{min}=40 Kbps).

In our method, the fairness causes the minimum rate be provided for each sensor.

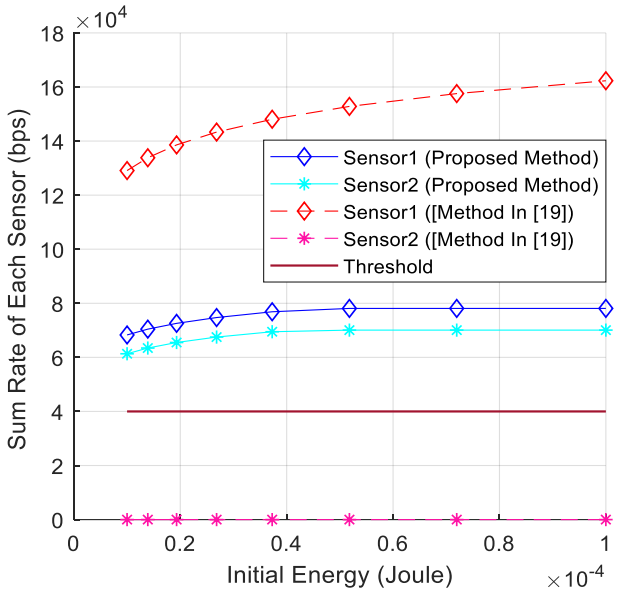

Fig. 9: Comparison of sum rate diagrams in terms of E_0 for proposed method and method of [19].

In Fig. 10, the AWST is plotted in terms of the initial energy E_0. In our method, compared to the method of [19], the value of obtained AWST is less because we have two more constraints, h, and l. Although AWST of [19] is higher than our method, it has two problems: First, fairness is not satisfied in [19], and second, buffers may overflow.

Therefore, the obtained AWST theoretically in [19] may not be achieved in practice.

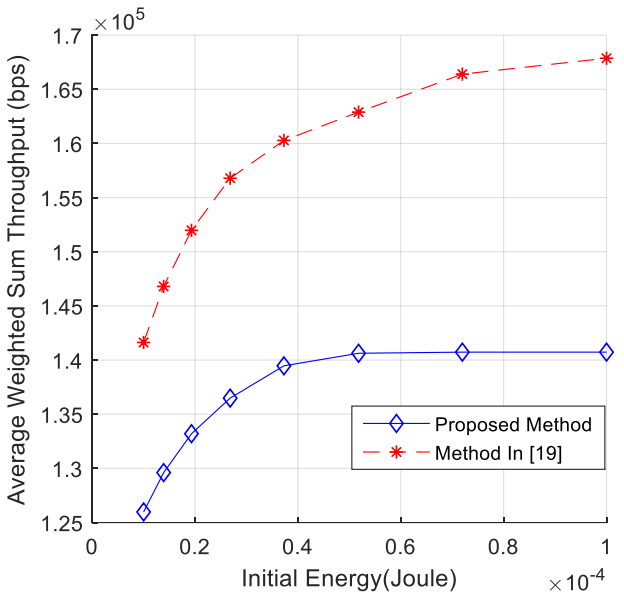

Fig. 10: Comparison of AWST diagrams in terms of E_0 for Proposed Method and Method of [19].

In Algorithm 1, the minimum rate, R_{min}, is a limiting condition that may make the problems infeasible in some channel conditions.

Therefore, we obtained the feasibility of the problems using Monte Carlo simulation by changing R_{min}, which can be seen in Fig. 11. This figure shows the effect of the minimum rate of sensors on the feasibility of the resource allocation problem. In Fig. 11, BF^{max}= 5 Kbit and the initial energy value E_0 is 10 microjoules. Resource allocation in the proposed method is more flexible than ETA mode. The first sensor has a higher rate due to a better channel, and a higher rate requires more power.

The buffer of both sensors is not negative as expected, and in addition, it remains smaller than its specified maximum value, which means that vital information is not lost. When the initial energy of the sensors is low at first, so they can send with less power, as a result, AWST is low. Different h_{rr} affects the channel capacity.

Increasing the h_{rr} reduces the capacity of the sensor channel to the relay, so the rate and consequently the AWST decreases.

In future work, the objective function can be the maximization of the energy efficiency or minimization of energy consumption. The relay can harvest energy from the body or RF signal. A system model can be considered, when the energy of one of the sensors is finished It sends an alert message in an uplink channel.

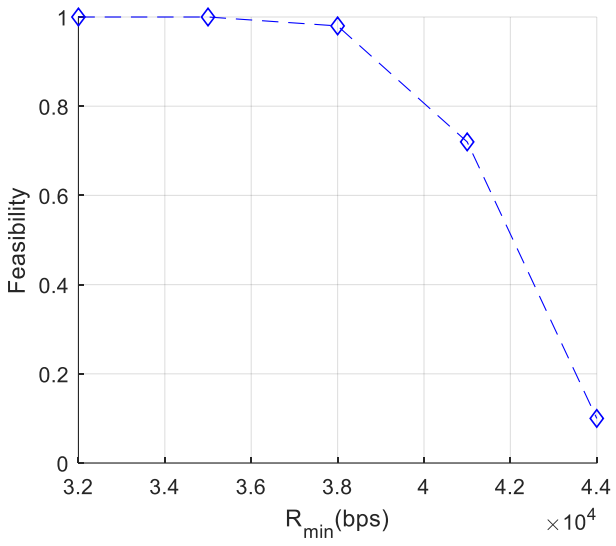

Fig. 11: The feasibility versus the minimum rate.

Conclusion

In this paper, a two-tier cooperative WBAN architecture including a FD relay, several sensors, and a destination were introduced was presented. In this system model, a coordinator based on the OA of time slots between sensors received the body's data from the sensors and simultaneously sent energy to them; it also sent sensors information to a destination, which is the AP here. In this system model, to face the problem of an energy shortage, the ability to harvest energy from the body was considered for the sensors. The purpose of this work is to maximize AWST with limited delay in the form of an MINLP and non-convex problem which included minimum data rate limit, energy limit, latency limit, and limited transmission power satisfaction. The goal of optimization can be to maximize energy efficiency or minimize energy consumption. In addition, the ability to command the sensors and having some actuators can be considered.

Author Contributions

All stages of research have been achieved with the participation, consensus, and equal efforts of both authors.

Acknowledgment

We thank reviewers for their so-called insights. We are also immensely grateful for their comments on an earlier version of the manuscript.

Conflict of Interest

The authors state that there is no obstacle and conflict of interest to publish this work. In addition, the ethical issues, including plagiarism, informed consent, misconduct, data fabrication and/or falsification, double publication and/or submission, and redundancy have been entirely and carefully witnessed by the authors.

Abbreviations

AP	*Access Point*
AWGN	*Additive White Gaussian Noise*
AWST	*Average Weighted Sum Throughput*
BEH	*Body Energy Harvesting*
ECG	*ElectroCardioGram*
DN	*Destination Node*
ETA	*Equal Time Allocation*
FD	*Full-Duplex*
FD-RN	*Full-Duplex Relay Node*
FIFO	*First-In-First-Out*
HD	*Half-Duplex*
KKT	*Karush–Kuhn–Tucker*
MILP	*Mixed-Integer Linear Programming*
MINLP	*Mixed-Integer Non Linear Programming*
OA	*Optimal Allocation*
QoS	*Quality of Service*
RF	*Radio Frequency*
RN	*Relay Node*
SI	*Self-Interference*
SN	*Sensor Node*
SWIPT	*Simultaneous Wireless Information and Power Transfer*
WBAN	*Wireless Body Area Network*
WPAN	*Wireless Personal Area Network*

References

[1] S. Li, F. Hu, Z. Mao, Z. Ling, Y. Zou, "Sum-throughput maximization by power allocation in WBAN with relay cooperation," IEEE Access, 7: 124727–124736, 2019.

[2] S. Movassaghi, M. Abolhasan, J. Lipman, D. Smith, A. Jamalipour, "Wireless body area networks : A survey," IEEE Commun. Surv. Tutorials, 16(3): 1658–1686, 2014.

[3] S. Dehghanpour, M. Majidi, "Simultaneous wireless information and power transfer in a network of on-body and implantable sensors with temperature constraint and intelligent channel prediction," Comput. Intell. Electr. Eng., 2021.

[4] A. Razavi, M. Jahed, "Capacity-outage joint analysis and optimal power allocation for wireless body area networks," IEEE Syst. J., 13(1): 635–646, 2019.

[5] X. Liu, F. Hu, M. Shao, D. Sui, G. He, "Power allocation for energy harvesting in wireless body area networks," China Commun., 14(6): 22–31, 2017.

[6] A. Vyas, S. Pal, B.K. Saha, "Relay-based communications in WBANs : A comprehensive survey," ACM Comput. Surv. (CSUR), 54(1): 1-34, 2020.

[7] M. Boumaiz, M. El Ghazi, S. Mazer, M. Fattah, A. Bouayad, M.E.l Bekkali, Y. Balboul, "Energy harvesting based WBANs: EH optimization methods," Procedia Comput. Sci., 151: 1040–1045, 2019.

[8] Z. Liu, B. Liu, C. Chen, C.W. Chen, "Energy-efficient resource allocation with QoS support in wireless body area networks," presented at the 2015 IEEE Global Communications Conference (GLOBECOM), San Diego, USA, 2015.

[9] H. Yektamoghadam, A. Nikoofard, "Fault detection in thermoelectric energy harvesting of human body," J. Electr. Comput. Eng. Innov., 9(1): 57–66, 2021.

[10] F. Akhtar, M.H. Rehmani, P. Design, "Energy harvesting for self-sustainable wireless body area networks," IT Prof., 19(2): 32–40, 2017.

[11] J.C. Kwan, A.O. Fapojuwo, "Radio frequency energy harvesting and data rate optimization in wireless information and power transfer sensor networks," IEEE Sens. J., 17(15): 4862–4874, 2017.

[12] L. Wang, F. Hu, Z. Ling, B. Wang, "Wireless information and power transfer to maximize information throughput in WBAN," IEEE Internet Things J., 4(5): 1663–1670, 2017.

[13] H. Gu, Z. Li, L. Wang, Z. Ling, "Resource allocation for wireless information and power transfer based on WBAN," Phys. Commun., 37, 2019.

[14] M. Mohammadkhani Razlighi, N. Zlatanov, "Buffer-aided relaying for the two-hop full-duplex relay channel with self-interference," IEEE Trans. Wirel. Commun., 17(1): 477–491, 2018.

[15] S. Shen, J. Qian, D. Cheng, K. Yang, G. Zhang, "A Sum-utility maximization approach for fairness resource allocation in wireless powered body area networks," IEEE Access, 7: 20014–20022, 2019.

[16] S. Li, F. Hu, J. Yu, Z. Huang, "Optimal power allocation with a cooperative relay in multi-point WBAN," presented at the IEEE/CIC International Conference on Communications in China (ICCC), Changchun, China, 2019.

[17] S. Li, F. Hu, Z. Xu, Z. Mao, Z. Ling, H. Liu, "Joint power allocation in classified WBANs with wireless information and power transfer," IEEE Internet Things J., 8(2): 989–1000, 2021.

[18] H. Liu, F. Hu, S. Qu, Z. Li, D. Li, "Multipoint wireless information and power transfer to maximize sum-throughput in WBAN with energy harvesting," IEEE Internet Things J., 6(4): 7069–7078, 2019.

[19] X. Zhang, K. Liu, L. Tao, "A cooperative communication scheme for full-duplex simultaneous wireless information and power transfer wireless body area networks," IEEE Sensors Lett., 2(4): 1–4, 2018.

[20] Z. Huang, Y. Cong, Z. Ling, Z. Mao, F. Hu, "Optimal dynamic resource allocation for multi-point communication in WBAN," IEEE Access, 8: 114153–114161, 2020.

[21] Y.H. Xu, G. Yu, Y.T. Yong, "Deep reinforcement learning-based resource scheduling strategy for reliability-oriented wireless body area networks," IEEE Sensors Lett., 5(1): 3–6, 2021

[22] Z. Liu, B. Liu, C. W. Chen, "Buffer-aware resource allocation scheme with energy efficiency and QoS effectiveness in wireless body area networks," IEEE Access, 5: 20763–20776, 2017.

[23] S. Boyd, L. Vandenberghe, Convex Optimization, United Kingdom: Cambridge, 2004.

[24] H. Zhang, S. Huang, C. Jiang, K. Long, V.C.M. Leung, H.V. Poor, "Energy-efficient user association and power allocation in millimeter-wave-based ultra-dense networks with energy harvesting base stations," IEEE J. Sel. Areas Commun., 35(9): 1936–1947, 2017.

[25] A.K. Shukla, P.K. Upadhyay, A. Srivastava, J.M. Moualeu, "Enabling co-existence of cognitive sensor nodes with energy harvesting in body," IEEE Sens. J., 21(9): 11213–11223, 2021.

[26] D. Sui, F. Hu, W. Zhou, M. Shao, M. Chen, "Relay selection for radio frequency energy-harvesting wireless body area network with buffer," IEEE Internet Things J., 5(2): 1100–1107, 2018.

[27] IEEE standard for local and metropolitan area networks part 15.6: Wireless body area networks, 2012.

[28] S. van Roy, F. Quitin, L. Liu, C. Oestges, F.Horlin, J.M. Dricot, P. De Doncker, "Dynamic channel modeling for multi-sensor body area networks," IEEE Trans. Antennas Propag., 61(4): 2200–2208, 2013.

[29] D. Cavalheiro, A.C. Silva, S. Valtchev, J.P. Teixeira, V. Vassilenko, "Energy harvested from the respiratory effort," presented at the 5th International Joint Conference on Biomedical Engineering Systems and Technology- BIOSTEC, Vilamoura, Portugal, 2012.

[30] E. Romero Ramirez, "Energy harvesting from body motion using rotational micro-generation," Ph.D. dissertation, Dept. Mech. Eng., Univ. Michigan Tech, 2010.

Biographies

Negarsadat Khatami received the B.SC. degree in biomedical engineering from the Islamic Azad University Khomeinishahr Branch, Isfahan, Iran, in 2014. She is graduated in the field of telecommunication engineering at the master's level of Kashan University, Isfahan, Iran, in 2020. Her research interests include wireless body area network (WBAN), optimization, and wireless powered communications.

- Email: negarsadat.khatami@grad.kashanu.ac.ir
- ORCID: NA
- Web of Science Researcher ID: NA
- Scopus Author ID: NA
- Homepage: NA

Mahdi Majidi received the B.Sc. degree in electrical engineering from Isfahan University of Technology, Isfahan, Iran, in 2004, and the M.S. and Ph.D. degrees in electrical engineering from Amirkabir University of Technology (Tehran Polytechnic), Tehran, Iran, in 2007 and 2014, respectively. In 2012, he joined the Communications and Networks Laboratory, Department of Electrical and Computer Engineering, National University of Singapore (NUS), Singapore, as a Visiting Ph.D. Student. In 2015, he worked as a researcher at the Iran Telecommunication Research Center (ITRC). Since 2016, he is an assistant professor of the Department of Electrical and Computer Engineering, University of Kashan, Iran. His research interests include numerical and analytical optimization methods, Intelligent reflecting surfaces, machine learning, wireless transceiver design, wireless powered communications, and multi-antenna communications.

- Email: m.majidi@kashanu.ac.ir
- ORCID: 0000-0003-0245-4738
- Web of Science Researcher ID: NA
- Scopus Author ID: 55512805400
- Homepage: https://faculty.kashanu.ac.ir/mmajidi/en

How to cite this paper:

N. Khatami, M. Majidi, "Resource allocation for full-duplex wireless information and power transfer in wireless body area network," J. Electr. Comput. Eng. Innovations, 10(2): 329-340, 2022.

DOI: 10.22061/JECEI.2021.8112.485

URL: https://jecei.sru.ac.ir/article_1638.html